

There was no problem related to the interface between the emitter and the embedded  $p^+$  layers. The technique employed here favours narrow-base HBTs.

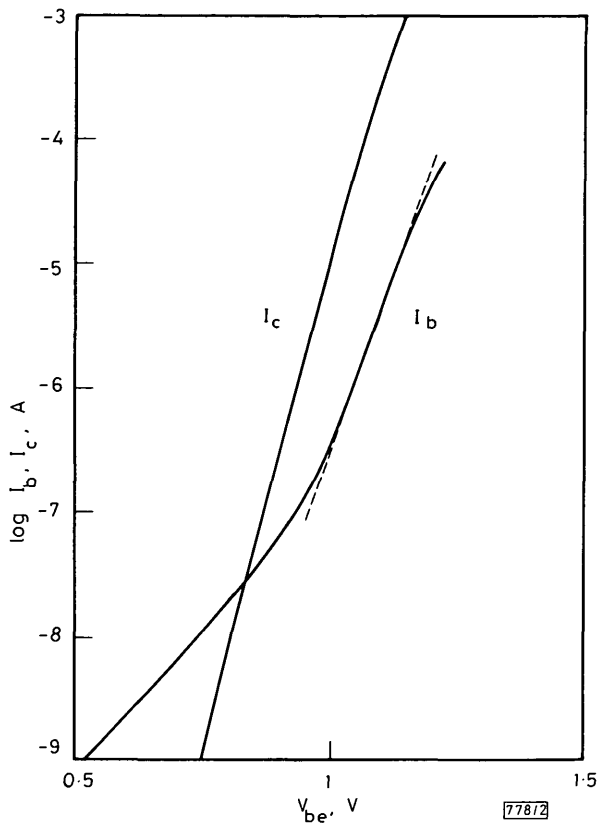


Fig. 2  $I_c$  and  $I_b$  against  $V_{be}$

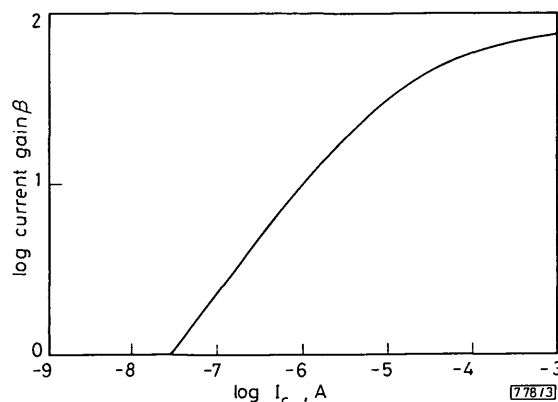


Fig. 3 Direct current gain  $\beta$  against  $I_c$

The authors wish to thank Miss Shimada for her assistance in device processing. They would also like to express their appreciation to C. Kojima, N. Watanabe and M. Kikuchi for their encouragement throughout this work.

K. TAIRA  
H. KAWAI  
K. KANEKO

21st July 1987

Sony Corporation Research Center  
174 Fujitsuka-cho, Hodogaya-ku  
Yokohama 240, Japan

References

- 1 ANKRI, D., and EASTMAN, L. F.: 'GaAlAs-GaAs ballistic heterojunction bipolar transistor', *Electron. Lett.*, 1982, 18, pp. 750-751
- 2 ASBECK, P. M., MILLER, D. L., BABCOCK, E. J., and KIRKPATRICK, C. G.: 'Application of thermal pulse annealing to ion-implanted GaAlAs/GaAs heterojunction bipolar transistors', *IEEE Electron Device Lett.*, 1983, EDL-4, pp. 81-84

FABRICATION AND PERFORMANCE OF 1.5 μm GaInAsP TRAVELLING-WAVE LASER AMPLIFIERS WITH ANGLED FACETS

Indexing terms: Semiconductor lasers, Optical amplifiers

A broadband 1.5 μm GaInAsP travelling-wave laser amplifier has been realised with angled facets instead of anti-reflection coatings. The measured signal gain for the TE mode is 19 dB at the wavelength around 1.49 μm with a 2 dB gain ripple over one free spectral range and a 3 dB bandwidth of 55 nm. The estimated residual modal reflectivity is 0.2%.

**Introduction:** Owing to its wide bandwidth and high saturation output power,<sup>1</sup> the travelling-wave amplifier (TWA) is very useful as an optical repeater and a preamplifier, especially in high-bit-rate and multichannel optical fibre transmission systems.<sup>2,3</sup> Current travelling-wave laser amplifiers rely on good antireflection coatings on both facets to prohibit the Fabry-Perot resonance. For example, to obtain a 30 dB internal gain with less than 3 dB gain ripple the facet reflectivity must be 0.01% or less, which requires extremely tight control on the refractive index and thickness of dielectric layers and can only be done one device at a time by a double-layer coating and *in situ* monitoring.<sup>4,5</sup>

A simpler way to suppress the Fabry-Perot resonance is to slant the waveguide (gain region) from the cleavage plane so that the internal light reflected by the cleaved facets does not couple back into the waveguide and is therefore lost (Fig. 1a). The reflectivity for the lowest-order TE mode decreases exponentially with the slant angle  $\theta_i$  (the angle between the waveguide axis and the normal of the cleaved facet).<sup>6</sup> High-power GaAs superluminescent diodes have been made with 5° inclination.<sup>7,8</sup> In this letter we report a broadband 1.5 μm GaInAsP travelling-wave laser amplifier with angled facets.

**Device fabrication and its far-field pattern:** Fig. 1 shows the TWA in a double-channel ridge-waveguide structure formed

by wet chemical etching<sup>9</sup> and oriented ~7° away from the [011] direction. The devices are fabricated on InP/GaInAsP double heterostructure wafers grown by LPE. The 1.5 μm active layer and the 1.3 μm antireflection layer are 0.26 μm thick in total and the ridge is 3.8-4.8 μm wide. The device is cleaved along the [011] direction into 500 μm lengths.

Fig. 2a shows the far-field patterns of a TWA in the junction plane, at various injection currents. The device with a

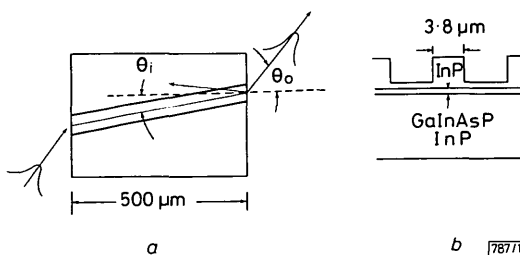


Fig. 1 Schematic drawings of travelling-wave laser amplifier with angled facets

a Top view  
b Cross-sectional view  
For conciseness, only ridge waveguide is shown in (a)

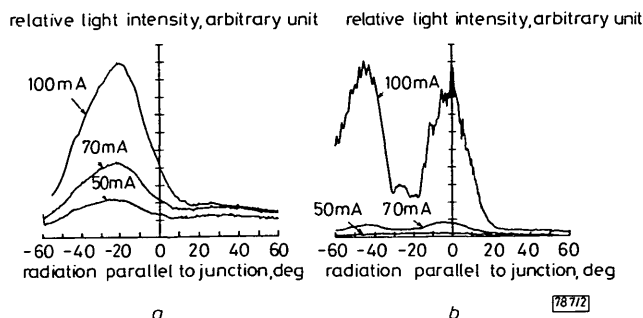


Fig. 2 Far-field patterns of devices with 7° angled facets in junction plane at various injection currents

a 3.8 μm-wide ridge  
b 4.8 μm-wide ridge

3.8  $\mu\text{m}$ -wide ridge does not lase and the peak intensity of the far-field pattern occurs at  $24^\circ$ , which corresponds to the refractive angle predicted by Snell's law with  $7^\circ$  incident angle. However, if the ridge is 4.8  $\mu\text{m}$  wide, which is wide enough to support high-order modes, the device lases with a threshold current of 85 mA and its far-field pattern shows two lobes, as in Fig. 2b. A detailed explanation of this effect will be presented elsewhere. Therefore, the narrower device is chosen to be the laser amplifier and its gain performance is described below.

**Gain measurement results:** The optical signal is generated from a DFB laser and modulated by a mechanical chopper. With synchronous detection including a large-area photodiode and lock-in amplifier, the amplified optical signal can easily be distinguished from the spontaneous emission. The input optical signal is coupled into the TWA along the direction of peak spontaneous emission intensity through a lensed single-mode fibre. For the convenience of coupling, a lensed multimode fibre aligned along the same direction is used at the output. The polarisation of the injected optical signal is controlled by a half-wave plate and a fibre polarisation controller. The fibre-to-fibre gain is taken as the ratio of lock-in amplifier outputs with and without the TWA. Since there is no anti-reflection coating on the facets, the reflection loss from the angled facet is estimated.<sup>10</sup> Table 1 lists measured fibre coupling losses and estimated facet reflection losses for both TE and TM modes. The measured fibre-to-fibre gain is corrected by the total loss in Table 1 to obtain the signal gain of the TWA.

**Table 1 FIBRE COUPLING LOSSES TO LASER AMPLIFIER WITH ANGLED FACETS**

	TE	TM
	dB	dB
Single-mode fibre coupling loss (input)	6.8	7.4
Multimode fibre coupling loss (output)	3.3	3.8
Reflection losses at facets	3.8	2.8
Total loss	13.9	14.0

Fig. 3 shows the signal gain of the TWA against current. Under a bias current of 125 mA, the signal gain at a wavelength of 1.49  $\mu\text{m}$  reaches 19 dB for the TE mode and 15 dB for the TM mode. The gain ripple of the TE mode at the same bias current is less than 2 dB over one free spectral range, measured by injecting an optical signal with a tunable wavelength around 1.494  $\mu\text{m}$ . The output saturation power is more than  $-3$  dBm, which is beyond our ability to test due to the available power launched into single-mode fibre from the DFB laser used in the experiment.

The TE-mode amplified spontaneous emission power spectrum at a bias current of 125 mA is shown in Fig. 4, and is normalised to the gain of 19 dB at 1.49  $\mu\text{m}$  measured by external optical injection. The maximum signal gain is about 20 dB at a wavelength of 1.475  $\mu\text{m}$ . The residual modal reflectivity is

about 0.2% as estimated by the 3 dB gain ripple at the maximum gain of 20 dB. The 3 dB gain bandwidth is 55 nm for the TE mode with a 20 dB signal gain, and 70 nm for the TM mode with a 16 dB signal gain.

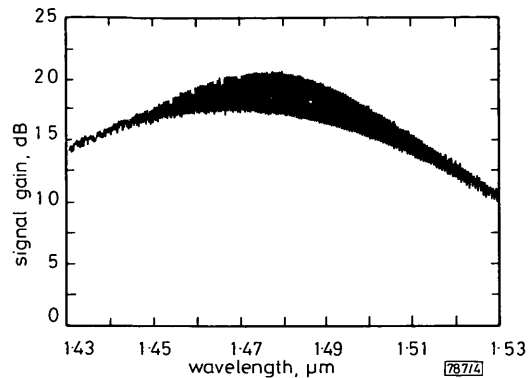


**Fig. 4 Power spectrum of TE-mode amplified spontaneous emission at 20 dB peak signal gain**

**Discussion:** We have demonstrated a broadband 1.5  $\mu\text{m}$  GaInAsP travelling-wave laser amplifier with angled facets instead of antireflection coatings. The residual modal reflectivity is estimated to be 0.2%, and this could be further reduced to 0.01% by applying  $\sim 1\%$  antireflection coatings on both facets, which is relatively easy to achieve. With such antireflection coatings, the fibre-to-fibre gain is expected to improve by about 4 dB for the TE mode and 3 dB for the TM mode. The signal gain undulation would also be reduced such that a higher signal gain could be obtained at higher bias currents. It is expected that a single-mode fibre-to-fibre gain of 10–15 dB is achievable. Since the angled facets can be fabricated in a batch process, the travelling-wave laser amplifier with angled facets is easier to reproduce than the one made with antireflection coatings alone.

**Acknowledgments:** The authors wish to thank F. Favire for packaging the devices and R. S. Vodhanel for providing the tunable laser.

C. E. ZAH  
J. S. OSINSKI  
C. CANEAU  
S. G. MENOCA  
L. A. REITH  
J. SALZMAN  
F. K. SHOKOOHI  
T. P. LEE

22nd July 1987

*Bell Communications Research, Inc.*  
331 Newman Springs Road  
Red Bank, NJ 07701, USA

## References

- SAITOH, T., and MUKAI, T.: 'Broadband 1.5  $\mu\text{m}$  GaInAsP travelling-wave laser amplifier with high-saturation output power', *Electron. Lett.*, 1987, **23**, pp. 218–219
- KOBAYASHI, S., and KIMURA, T.: 'Semiconductor optical amplifiers', *IEEE Spectrum*, May 1984, pp. 26–33
- MUKAI, T., INOUE, K., and SAITOH, T.: 'Signal gain saturation in two-channel common amplification using a 1.5  $\mu\text{m}$  InGaAsP travelling-wave laser amplifier', *Electron. Lett.*, 1987, **23**, pp. 396–397
- SAITOH, T., and MUKAI, T.: 'Theoretical analysis and fabrication of antireflection coatings on laser-diode facets', *J. Lightwave Technol.*, 1985, **LT-3**, pp. 288–293
- SERENYI, M., and HABERMEIER, H.-U.: 'Directly controlled deposition of antireflection coatings for semiconductor lasers', *Appl. Opt.*, 1987, **26**, pp. 845–849
- SCIFRES, D. R., STREIFER, W., and BURNHAM, R. D.: 'GaAs/GaAlAs diode lasers with angled pumping stripes', *IEEE J. Quantum Electron.*, 1978, **QE-14**, pp. 223–227
- ALPHONSE, G. A., GILBERT, D. B., HARVEY, M., DEPIANO, E., and ETTEMBERG, M.: 'High-power superluminescent diodes'. *OFC/IOOC*, Reno, Nevada, 1987, Paper ME6
- NIESEN, J., PAYTON, P. H., MORRISON, C. B., and ZINKIEWICZ, L. M.: 'High power 0.83  $\mu\text{m}$  angle stripe superluminescent diode'. Southwest optics conference, Albuquerque, New Mexico, 1987, Paper Tuc-1

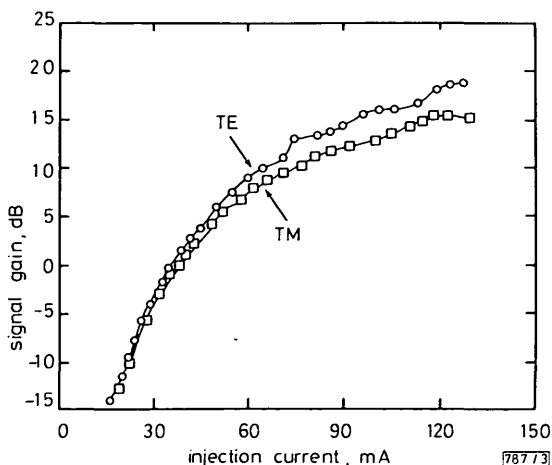


**Fig. 3 Signal gain of TWA against currents at 1.49  $\mu\text{m}$**

- 9 KAMINOW, I. P., STULZ, L. W., KO, J.-S., MILLER, B. I., FELDMAN, R. D., DEWINTER, J. C., and POLLACK, M. A.: 'Low threshold ridge waveguide laser at 1.55  $\mu\text{m}$ ', *Electron. Lett.*, 1983, **19**, pp. 877-879
- 10 Ikegami, T.: 'Reflectivity of mode at facet and oscillation mode in double-heterostructure injection lasers', *IEEE J. Quantum Electron.*, 1972, **QE-8**, pp. 470-476

## CHIRP-INDUCED PENALTY IN OPTICAL FIBRE SYSTEMS

*Indexing terms: Optical communications, Laser chirp, Optical modulation*

Using the output light intensity and wavelength chirp waveforms obtained with a SPICE2 equivalent circuit laser model, together with a computer model for chirp-dispersion interaction, the chirp-induced power penalty is estimated. In contrast with previously published theoretical estimates, the results obtained show good agreement with reported experiments.

**Introduction:** Direct modulation of an injection laser diode produces fluctuation of the emitted optical wavelength. This results in data-dependent distortion in long-haul, high-bit-rate, direct-detection optical communication systems due to interaction with the generally nonzero chromatic dispersion of monomode fibres. Theoretical estimates of the resulting penalty published to date<sup>1-3</sup> have made use of severe simplifying assumptions concerning laser dynamics and have proved to be unduly pessimistic, when compared with reported experimental results.<sup>4</sup> For example, the results obtained by Koch and Bowers<sup>2</sup> were based on Gaussian optical pulses with a linear chirp, but in practice the optical pulses are far from being Gaussian and have much sharper leading and trailing edges. Even the so-called super-Gaussian pulses, proposed by Agrawal and Potasek<sup>3</sup> as a more realistic model, do not account for the laser's relaxation oscillation and for the use of different biasing conditions.

This letter outlines a simulation strategy which takes into account laser dynamics, using the common circuit analysis program SPICE2<sup>5</sup> to model the laser diode (LD). A numerical technique is employed to calculate the distorted signal waveforms at the input to the receiver filter, considering the interaction between chirp and fibre dispersion.

**Modelling:** The LD model is broadly similar to that outlined by Tucker,<sup>6</sup> and is obtained by combining a network representing package and chip parasitics with the large-signal circuit model of the intrinsic laser, obtained from a pair of single-mode rate equations which incorporate optical field-dependent gain saturation. The more relevant intrinsic device parameters and parasitic elements used in the model are presented in Tables 1 and 2.

The input is the drive current  $I$  and the outputs are the emitted optical power  $P$  and wavelength chirp  $\Delta\lambda$ . The drive circuit is modelled by a current source with internal resistance (1 k $\Omega$  in our studies) representative of the output impedance of FET or bipolar transistor drivers. The model was 'biased'

**Table 1** INTRINSIC LASER PARAMETERS

Parameter	Value
Active volume $V_a$	$90 \times 10^{-18} \text{ m}^3$
Spontaneous emission factor $\beta$	$4 \times 10^{-4}$
Optical confinement factor $\Gamma$	0.44
Optical gain slope constant $g_0$	$3 \times 10^{-12} \text{ m}^3 \text{ s}^{-1}$
Optical gain compression factor $\epsilon$	$3.4 \times 10^{-23} \text{ m}^3$
Linewidth enhancement factor $\alpha$	5
Differential quantum efficiency $\eta$	0.1
Carrier density at $g = 0$ , $N_0$	$1.2 \times 10^{24} \text{ m}^{-3}$
Carrier lifetime $\tau_n$	3 ns
Photon lifetime $\tau_p$	1 ps
Emission wavelength $\lambda_0$	1502 nm
Threshold voltage $V_{th}$	0.9 V
Space-charge capacitance $C_{sc}$	0.3 pF

slightly above threshold ( $I_b = 1.1I_{th}$ ), with the peak drive current approximately twice the bias current.

As an illustrative test signal, a pseudorandom maximum-length NRZ 15-bit sequence was used, and zeros were appended to this sequence to account for the pulse spreading due to dispersion and the relatively long turn-off time of the LD. The resultant optical power and chirp profiles obtained with SPICE2 for a bit rate ( $B$ ) of 4 Gbit/s are shown in Fig. 1. The optical power is normalised and the wavelength shift is referred to the on-state emission wavelength.

**Table 2** PARASITIC ELEMENTS

Parasitic	Value
Bond-wire resistance $R_p$	0.2 $\Omega$
Bond-wire inductance $L_p$	2 nH
Standoff shunt capacitance $C_p$	0.1 pF
Total series resistance $R_s$	3 $\Omega$
Shunt parasitic capacitance $C_s$	11.3 pF
Substrate resistance $R_{sub}$	0.5 $\Omega$
DC leakage $I_l$	10 mA

The distorted optical power waveform at the input to the receiver filter is obtained using the chirp profile to effect a nonlinear transformation of the time axis, as proposed by Frisch and Henning,<sup>7</sup> the time axis  $t$  of the emitted waveform changing to an  $s$ -axis,  $s = t + k \Delta\lambda(t)$ , where  $k$  is the time dispersion for the system of interest.

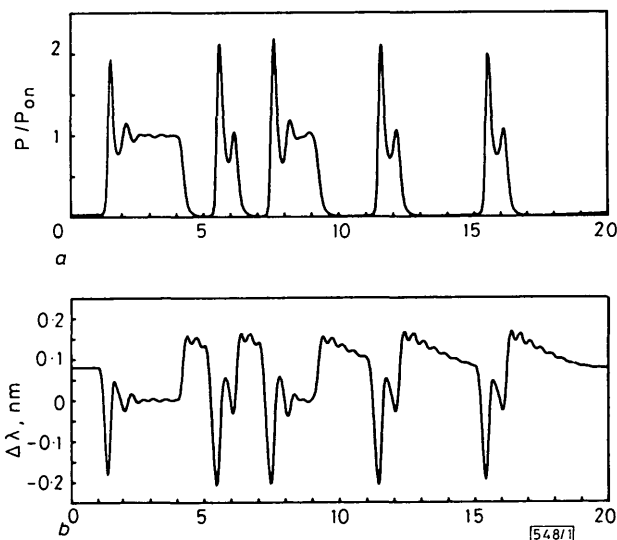


**Fig. 1** (a) Normalised optical power  $P/P_{on}$  and (b) wavelength chirp  $\Delta\lambda = \lambda - \lambda_{on}$  obtained with SPICE2 for a pseudorandom sequence at  $B = 4 \text{ Gbit/s}$

At the receiver, a raised-cosine filter modified for a rectangular input pulse with duration  $T = 1/B$  is assumed. The filtered eye diagrams obtained without dispersion ( $k = 0$ ) and with  $k = 2 \text{ ns/nm}$  (approximately 100 km of standard monomode fibre) are shown in Fig. 2. The eye closure due to chirp-dispersion interaction is evident.

**Chirp-induced penalty:** The chirp-induced dispersion penalty was calculated from the eye diagrams, using as a reference the eye opening in the absence of dispersion. Decision sampling times were optimised to make use of the maximum eye opening.

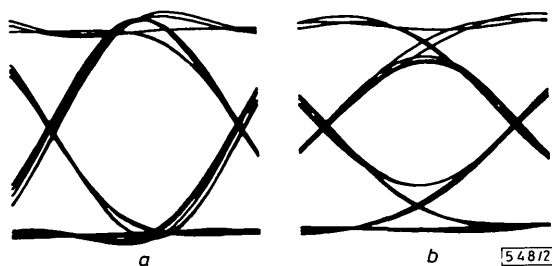


**Fig. 2** Filtered eye diagrams received (a) without dispersion ( $k = 0$ ) and (b) with system dispersion  $k = 2 \text{ ns/nm}$